Iterative Demodulation and Decoding of Coded Non-Square QAM

Lifang Li, Dariush Divsalar, Samuel Dolinar
Jet Propulsion Laboratory
California Institute of Technology
Pasadena, CA 91109-8099, USA

MILCOM'03 PTN: No. 1025

Abstract

It is shown that a non-square (NS) 2^{2n+1}-ary quadrature amplitude modulation (QAM) can be decomposed into a single-parity-check (SPC) block encoder and a memoryless modulator in such a way that the inherent block encoder has a recursive nature. When concatenated with a forward-error-correcting (FEC) code, iterative demodulation and decoding of the FEC code and the inherent SPC code of NS-2^{2n+1}-QAM is then possible. The capacity and bit/symbol-error-rate (BER/SER) performance of coded and uncoded NS-2^{2n+1}-QAM systems are given and compared to those of other 2^{2n+1}-ary systems. Simulation results show that, with iterative demodulation and decoding, coded NS-8QAM performs 0.5 dB better than standard 8QAM and 0.7 dB better than 8PSK at BER= 10^{-5}, when the FEC code is the $(15, 11)$ Hamming code concatenated with a rate-1 accumulator code, while coded NS-32QAM performs 0.25 dB better than standard 32QAM.

I. Introduction

Shortly after the introduction of the revolutionary turbo codes consisting of parallel concatenated convolutional codes (PCCC) in 1993 [1], serially concatenated codes (SCC) were shown to have comparable performance [2], [3]. Later it has been realized that some modulation schemes have inherent memory, which could be made explicit and serve as an inner code in a coded system with iterative decoding. Such modulation schemes include continuous phase modulation (CPM) [4]–[7], differential phase shift keying (DPSK), and Differential quaternary phase shift keying (DQPSK) [8]–[10]. It was shown that the inherent recursive convolutional code of these modulation schemes combined with an interleaver significantly improves the distance spectrum of the transmitted signals and therefore yields large coding gains [10]. Another modulation scheme that has memory is Feher-patented QPSK (FQPSK) [11].

This work was performed at the Jet Propulsion Laboratory, California Institute of Technologyi, under a contract with the National Aeronautics and Space Administration.

By using a representation of FQPSK as a trellis coded modulation, large coding gains are achievable even when simple outer codes are used [12]–[14].

In applications that require high bandwidth efficiency, high-order modulation schemes such as M-ary quadrature amplitude modulation (QAM) ($M > 4$) are often considered. In this paper we will show that a non-square (NS) 2^{2n+1}-QAM ($n = 1, 2, \ldots$) also has inherent memory.In other words, NS-2^{2n+1}-QAM is by itself a form of coded modulation. Specifically, we will show that NS-2^{2n+1}-QAM can be decomposed into a $(2n+2, 2n+1)$ single-parity-check (SPC) encoder and a memoryless modulator, where independent inphase (I) and quadrature (Q) signal mapping is possible. Fig. 1 gives the block diagram of a coded system with NS-2^{2n+1}-QAM modulation. In this figure, input data is first encoded by a forward-error-correcting (FEC) encoder. The encoded bits are then permuted by a random interleaver π before every $2n+1$ bits are mapped into an NS-2^{2n+1}-QAM symbol. It will be shown in Section II that the mapping process is equivalent to the following. First, the $2n+1$ bits are passed through a $(2n+2, 2n+1)$ SPC encoder. Then the $2n+2$ output bits are evenly divided into two groups. Each group of $n+1$ output bits is mapped to a 2^{n+1}-ary pulse amplitude modulation (PAM) symbol. The two 2^{n+1}-PAM symbols are then transmitted through the I and Q channels independently.

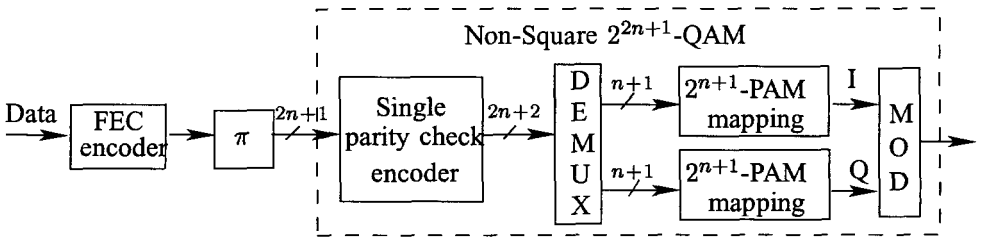

Fig. 1. A coded system with NS-2^{2n+1}-QAM.

We will show that this decomposition of NS-2^{2n+1}-QAM can be applied to obtain joint iterative demodulation and decoding algorithms in a coded system that explore the inherent memory of NS-2^{2n+1}-QAM and achieve better coding gains. In addition, the decoding complexity can be reduced to that of 2^{n+1}-PAM systems. In practice, we will see that NS-2^{2n+1}-QAM can be implemented by using existing 2^{2n+2}-QAM hardware directly, since its signal constellation is just a subset of the 2^{2n+2}-QAM square constellation. We will then compare the capacity and bit/symbol-error-rate (BER/SER) performance of coded and uncoded NS-2^{2n+1}-QAM systems with those of other 2^{2n+1}-ary modulation schemes. Simulation results show that, with iterative demodulation and decoding, coded NS-8QAM performs 0.5 dB better than standard 8QAM and 0.7 dB better than both 8PSK and star-8QAM at BER$= 10^{-5}$ when the FEC code is the $(15, 11)$ Hamming code concatenated with a rate-1 accumulator code [15], while coded NS-32QAM performs 0.25 dB better than standard 32QAM.

The remainder of the paper is organized as follows. In Section II we show the decomposition of NS-2^{2n+1}-QAM and the recursive convolutional nature of its inherent SPC code. We describe the iterative demodulation and decoding process of coded NS-2^{2n+1}-QAM systems in Section III, using as an example a novel serially concatenated code

composed of (15,11) Hamming outer codes and rate-1 accumulator inner codes. The capacity and uncoded system performance comparisons of NS-2^{2n+1}-QAM and other 2^{2n+1}-ary schemes are given in Section IV. In Section V we present simulation results of coded NS-2^{2n+1}-QAM system performance and compare them to those of other 2^{2n+1}-ary systems. Finally, our conclusions are given in Section VI.

II. Decomposition of NS-2^{2n+1}-QAM

We study the NS-2^{2n+1}-QAM constellation as proposed in [16]. To obtain this NS-2^{2n+1}-QAM constellation, we start with the square constellation for 2^{2n+2}-QAM with independent I-dimension and Q-dimension Gray-code (GC) mapping[1]. That is, each dimension of the square 2^{2n+2}-QAM is an independent 2^{n+1}-PAM with GC mapping. There are 2^{2n+2} signal points in the square 2^{2n+2}-QAM constellation. The GC label of each signal point can be easily obtained by concatenating its I-dimension GC label with its Q-dimension GC label. Now by deleting every other point in each dimension, we have only half of the points left in each row and half of the points left in each column. The remaining points in each row have the same distance between them, and so do the remaining points in each column. The total number of remaining points is 2^{2n+1} and these points form the non-square constellation for NS-2^{2n+1}-QAM. Fig. 2 and Fig. 3 show the resulting non-square constellations of NS-8QAM ($n = 1$) and NS-32QAM ($n = 2$), respectively.

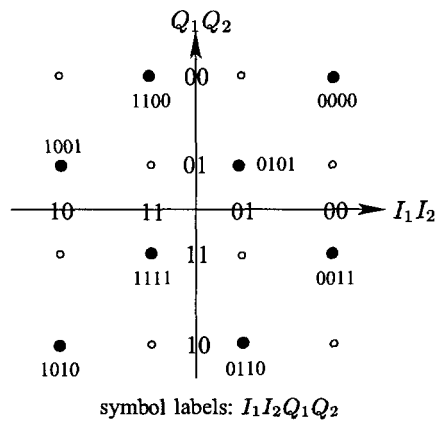

Fig. 2. NS-8QAM signal constellation.

Now instead of re-labeling the 2^{2n+1} points as shown in [16], we keep their labels unchanged. That is, the labels for these remaining 2^{2n+1} points are the same as in the square 2^{2n+2}-QAM constellation. This means that $2n+2$ bits are used to label each of the 2^{2n+1} points in the NS-2^{2n+1}-QAM constellation: $n+1$ bits (denoted as $I_1, \ldots, I_{n+1}$) for the I-dimension labeling, and $n+1$ bits (denoted as $Q_1, \ldots, Q_{n+1}$) for the Q-dimension labeling. However, we know that each point in a 2^{2n+1}-QAM constellation only represents $2n+1$ bits of information. Therefore, the

[1]Other kinds of mapping are also applicable if desired.

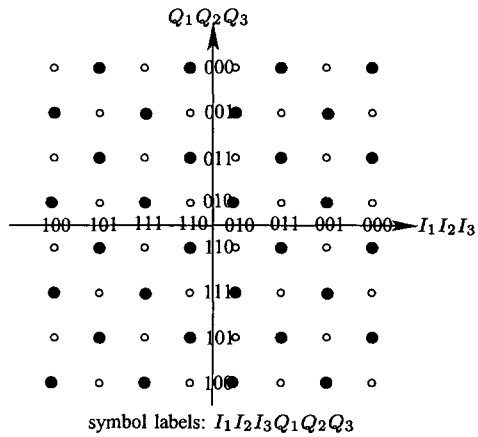

Fig. 3. NS-32QAM signal constellation.

$2n+2$ bits used for labeling an NS-2^{2n+1}-QAM signal point are not independent. Close examinations show that, for any signal point in the NS-2^{2n+1}-QAM constellation, the last bit of its $2n+2$ labeling bits can be viewed as apar ity-check bit of the other $2n+1$ bits. In other words, if we label an NS-2^{2n+1}-QAM signal point as $I_1 \ldots I_{n+1} Q_1 \ldots Q_{n+1}$, then

$$Q_{n+1} = \left(\sum_{i=1}^{n+1} I_i + \sum_{i=1}^{n} Q_i \right) \mod 2. \tag{1}$$

For example, when $n = 1$ and an NS-8QAM single point is labeled as $I_1 I_2 Q_1 Q_2$, then $Q_2 = I_1 \oplus I_2 \oplus Q_1$, where $\oplus$ denotes "exclusive OR" operation. This can be easily verified for symbol labels shown in Fig. 2.

Therefore, each NS-2^{2n+1}-QAM symbol can be generated by first encoding the corresponding $2n+1$ bits with a $(2n+2, 2n+1)$ SPC block encoder and then using the $2n+2$ encoded bits to select one of the $2n+1$ points on the NS-2^{2n+1}-QAM constellation. Specifically, the I-dimensional position and the Q-dimensional position of a signal point on an NS-2^{2n+1}-QAM constellation can be independently determined by the first $n+1$ encoded bits and the remaining $n+1$ encoded bits, respectively.

Similar to the convolutional encoding of the (n, k) Hamming code in [15], the $(2n+2, 2n+1)$ SPC block code can be generated as a recursive, systematic, terminated convolutional code with two states. The convolutional encoder structure of this SPC code is shown in Fig. 4. From this figure it is clear that, since the feed-forward bit from the shift register is the same as the feedback one, the encoded output bits at point D will always be the same as the input bits at point C. For the first input $2n+1$ bits, the switch in Fig. 4 is connected to point A and the $2n+1$ input bits at point A will emerge as the first $2n+1$ encoded bits. After the $2n+1$ bits, the switch in Fig. 4 is toggled to point B to produce an additional encoded bit. This additional bit will be the same as the feedback bit, which is the parity-check bit for the previous $2n+1$ bits.

Although it is easily seen that each signal point on the NS-2^{2n+1}-QAM constellation can be uniquely determined and labeled with the $2n+1$ input bits only (i.e., without the parity-check bit Q_{n+1}), there are two obvious advantages

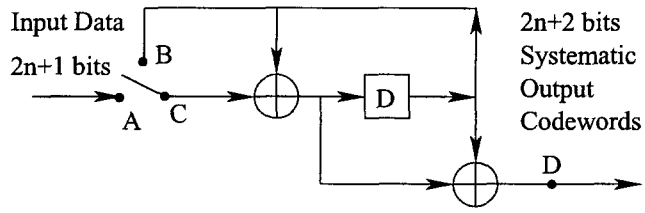

Fig. 4. A recursive convolutional structure for SPC encoder.

for the decomposition of the NS-2^{2n+1}-QAM into a recursive convolutional encoder and a memoryless modulator with independent I-dimension and Q-dimension GC mapping. First, when NS-2^{2n+1}-QAM is used in a coded system, the decomposition can be applied to obtain optimum demodulation and decoding algorithms so as to achieve better coding gains. The second obvious advantage is that, when performing iterative demodulation and decoding, the computational complexity for determining the log-likelihood ratio (LLR) of each bit is reduced dramatically due to the independent I-dimension and Q-dimension mapping/demapping of the NS-2^{2n+1}-QAM signals. In particular, for a coded M-ary modulation system, if independent I and Q mapping/demapping are not possible, computing the LLR for each bit of a signal point with a received symbol requires calculating the distance between the received symbol and each of the M points on the M-ary signal constellation. That is, M distinct Euclidian distances have to be calculated and compared for each bit with a given received symbol. However, in the case of independent Iand Q mapping/demapping, since each bit of a signal point is only involved in one dimensional mapping/demapping, computing its LLR with a received symbol is now equivalent to that of a one-dimensional modulation system. For example, since the NS-2^{2n+1}-QAM signal mapping can be decomposed into two independent 2^{n+1}-PAM mapping (one in each dimension), computing the LLR for each bit only requires calculating 2^{n+1} Euclidian distances in a single dimension instead of 2^{2n+1} distances in two dimensions. More details about the iterative demodulation and decoding procedure will be given in Section III.

III. Iterative Demodulation and Decoding

We now consider the case where the FEC scheme in Fig. 1 is a serial concatenation of the high-rate $(15, 11)$ Hamming outer code and a simple two-state rate-1 accumulator inner code, separated by a novel "parallel interleaver" that allows decoding with a parallel architecture at very high speeds, on the order of 1 Gbps [15]. When combined with NS-2^{2n+1}-QAM, it can achieve a bandwidth efficiency of $(2n+1) \times \frac{11}{15}$ bits/sec/Hz (or bps/Hz).

The encoder structure of this concatenated code is shown in Fig. 5. In this figure, there are 372 parallel Hamming encoders and 15 parallel accumulating encoders. The block interleaver in the middle has 372 rows and 15 columns. There is a random interleaver π of size 15 following each Hamming encoder. It permutes the 15 output bits of the Hamming encoder before they are written into the corresponding row of the block interleaver. Each of the 372 random interleavers has a distinct permutation pattern. The data in the block interleaver are read out column by column. Before the data in each column are encoded by an accumulating encoder, they are permuted by a random

interleaver π of size 372. There are 15 such random interleavers and each of them also has a distinct permutation pattern. This encoder structure yields an overall code of length 5580 (15×372) and dimension 4092 (i.e., there are 11×372 input bits).

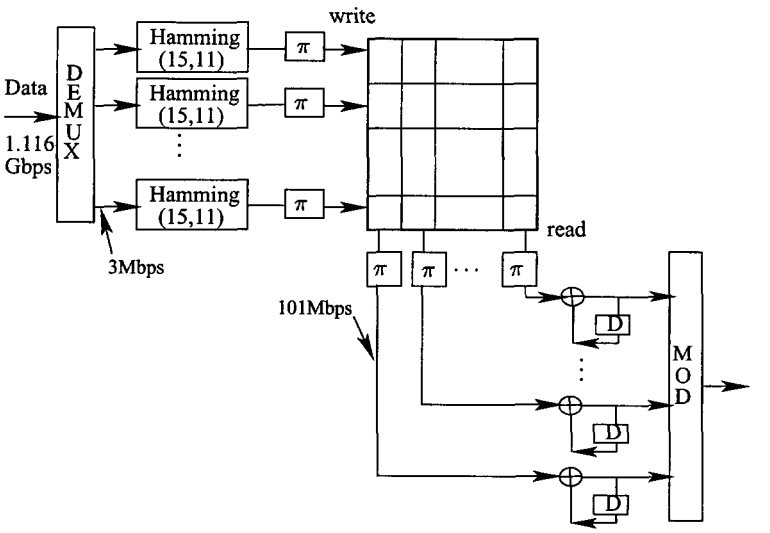

Fig. 5. Encoder structure for the Hamming and accumulator code.

In this figure we indicate that adesired input data rate of 1.116 Gbps can be obtained by running the 372 Hamming encoders at 3 Mbps each, and the 15 accumulating encoders at 101 Mbps each. The outputs of the 15 accumulating encoders are mapped into NS-2^{2n+1}-QAM signal points. With NS-8QAM the first output bits of the first three accumulators are used to choose one of the 8 signal points on the non-square constellation as shown in Fig. 2. Then the first output bits of the next three accumulators are used to choose the second NS-8QAM symbol and so on, until the first five NS-8QAM symbols are produced. Then the next five NS-8QAM symbols are created using the second bits from three accumulators at a time, and so forth. With NS-32QAM we take output bits five at a time from five separate accumulators to form each NS-32QAM symbol, stepping through the 15 accumulator codes in a cyclic order until all 5580 output bits are mapped. This type of mapping eliminates the need for a channel interleaver.

We now show how to perform iterative demodulation and decoding when this serially concatenated Hamming and accumulator code is combined with the proposed NS-2^{2n+1}-QAM to achieve good power and bandwidth efficiency at very high decoding rate. Fig. 6 shows the decoder structure for the three serially concatenated codes: the inherent SPC code of NS-2^{2n+1}-QAM, the accumulator code, and the Hamming code. Note that each of the three constituent codes has a time-invariant trellis representation due to its recursive convolutional structure. The soft-input soft-output (SISO) module [17], [18] applying the Bahl-Cocke-Jelinek-Raviv (BCJR) algorithm [19] on a time-invariant trellis is used to decode each constituent code.

Specifically, in this figure, given the received I and Q channel observations for each symbol, the reliabilities

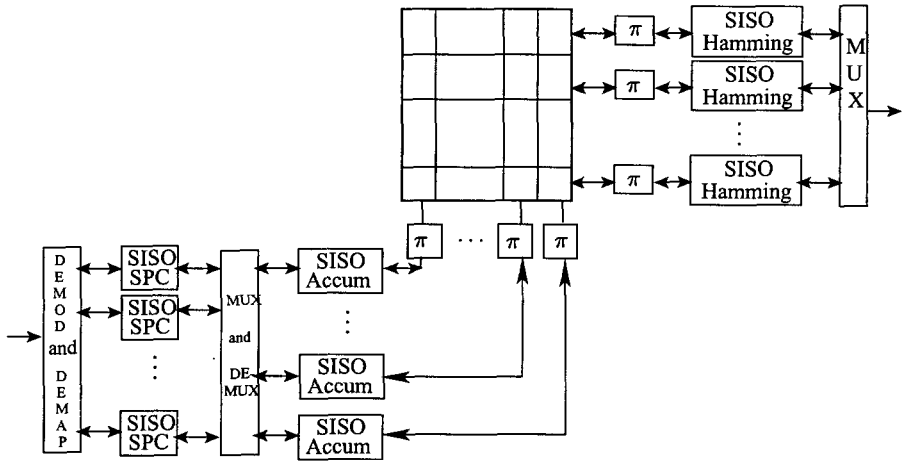

Fig. 6. Decoder structure for the inherent SPC code and the Hamming and accumulator code.

(or LLRs) for the $n+1$ bits (i.e., $I_1, \ldots, I_{n+1}$) assigned to I-dimension labels of an NS-2^{2n+1}-QAM symbol are calculated based on the I channel observations only, and the reliabilities for the other $n+1$ bits (i.e., $Q_1, \ldots, Q_{n+1}$) assigned to Q-dimension labels are calculated based on the Q channel observations only. The observation-based reliabilities for all $2n+2$ bits (i.e., $I_1, \ldots, I_n+1, Q_1, \ldots, Q_{n+1}$) provided by the I and Q demappers as well as the properly demultiplexed extrinsic information for all bits but Q_{n+1} from the accumulator SISO modules are used in the SISO module for the SPC code. For the $(2n+2, 2n+1)$ systematic SPC code, the first $2n+1$ bits (i.e., $I_1, \ldots, I_{n+1}, Q_1, \ldots, Q_n$) are just information bits, which means they are direct output bits of the accumulators. Therefore, after being properly multiplexed and demultiplexed, the observation-based reliabilities for these $2n+1$ bits will be used directly in the SISO modules for the accumulator codes. In addition, there is still extrinsic information from the SISO module of the SPC code for these $2n+1$ bits. In this case, care must be taken when calculating such extrinsic information. In particular, for the length $2n+2$ SPC code, the extrinsic information for each of its first $2n+1$ bits should now be derived from all observation-based reliabilities but that of itself, instead of from all $2n+2$ reliabilities including that of itself. Details on essential information exchange between SISO modules for serially concatenated convolutional codes are clarified in [20].

IV. Capacity and Uncoded System Performance Comparison

In this section we will compare the capacity of the proposed NS-2^{2n+1}-QAM (n=1, 2) on additive white Gaussian noise (AWGN) channels with that of other 2^{2n+1}-ary signal constellations. We will also compare the SER of uncoded NS-2^{2n+1}-QAM (n=1, 2) systems with that of other 2^{2n+1}-ary systems. For NS-32QAM, we compare its performance with that of standard 32QAM, the constellation of which has the "central-square-with-four-wings" structure [21]. For NS-8QAM, we compare its performance with that of standard 8QAM, star-8QAM, and 8PSK. Fig. 7 shows the constellations for standard 8QAM and star-8QAM. This star-8QAM was considered to be the best 8QAM in [22] since it offers the largest "minimum distance to average power" ratio.

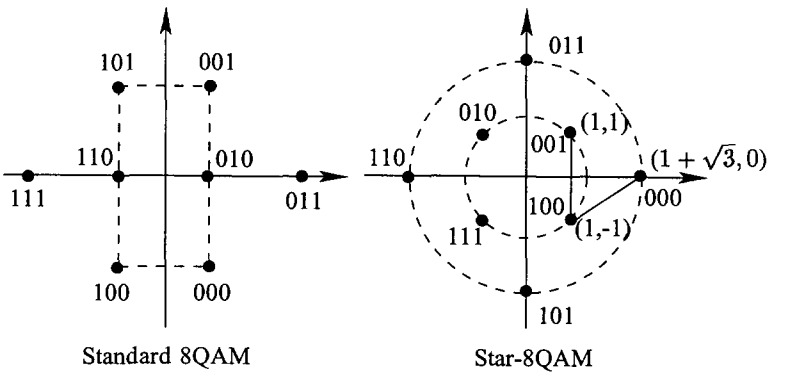

Fig. 7. Standard 8QAM and star-8QAM signal constellations.

Note that although labeled differently, the standard 8QAM constellation is essentially the same as that of NS-8QAM, if we rotate it counter-clockwise by 45°. Therefore, these two 8QAM schemes will have the same capacity and the same SER in an uncoded system.

A. Symbol Error Rate

Since it is hard to derive the exact SER for these modulation schemes, for comparison purposes we compute their approximate upper bounds. For a given signal constellation, assuming maximum-likelihood detection and large signal-to-noise ratio (SNR), the approximate upper bound for the SER P_e can be expressed as [23]:

$$P_e \leq c_1 \cdot \mathrm{erfc}\left(\sqrt{c_2 \frac{E_b}{N_0}}\right), \tag{2}$$

where c_1 and c_2 are constants determined by the constellation, erfc(·) is the complementary error function, and E_b/N_0 is the SNR per bit. Note that c_2 is proportional to the "minimum distance to average power" ratio of the constellation. It can be easily computed that, for star-8QAM, $c_1 = \frac{3}{2}$, $c_2 = \frac{3-\sqrt{3}}{2} \simeq 0.634$; for both standard 8QAM and NS-8QAM, $c_1 = \frac{9}{8}$, $c_2 = \frac{3}{5} = 0.6$; for 8PSK, $c_1 = 1$, $c_2 = 3\sin^2(\frac{\pi}{8}) \simeq 0.439$; for standard 32QAM, $c_1 = \frac{13}{8}$, $c_2 = \frac{3}{20} = 0.15$; and for NS-32QAM, $c_1 = \frac{49}{32}$, $c_2 = \frac{3}{21} \simeq 0.143$.

Fig. 8 shows this upper bound for the six different modulation schemes. From this figure we see that, for large E_b/N_0, star-8QAM does perform slightly better than NS-8QAM and standard 8QAM. In addition, all three 8QAM schemes have much better SER than 8PSK, as expected. In the 32QAM case, standard 32QAM performs slightly better than NS-32QAM.

B. Capacity

We use the method described in [24] to calculate the capacity or bandwidth efficiency in bits/sec/Hz for the six different modulation schemes. Fig. 9 shows the numerical results. In this figure, we see that all three 8QAM schemes have obviously larger capacity than 8PSK. However, the capacity of NS-8QAM and standard 8QAM is slightly larger than that of star-8QAM, though the uncoded star-8QAM has better SER, as shown in Fig. 8. For 32QAM,

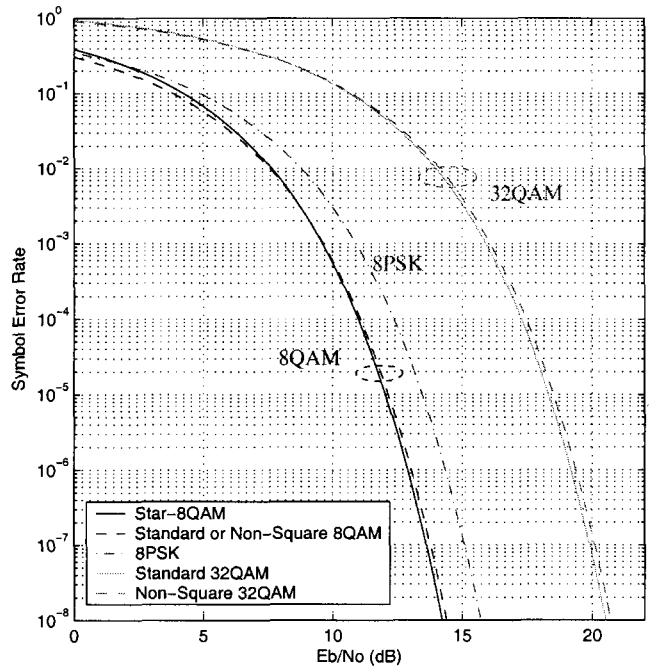

Fig. 8. SER upper bounds for the six uncoded modulation schemes.

standard 32QAM constellation yields a slightly larger capacity than the NS-32QAM one, though the difference is negligible.

V. Coded System Performance Comparison

In this section we show simulation results for the six coded systems, where the FEC code is the (15,11) Hamming code concatenated with the accumulator code, as shown in Section III. Fig. 10 shows the BER of four different 8-ary systems with iterative decoding: NS-8QAM, standard 8QAM, star-8QAM, and 8PSK. For NS-8QAM, the iterative demodulation and decoding procedure as described in Section III is applied. For the other three 8-ary systems, iterative decoding of the Hamming code and of the accumulator code using the standard BCJR algorithm is performed after demodulation.

Since GC labeling is impossible for 2^{2n+1}-QAM ($\forall n \geq 1$) [21], in our simulations we have adopted a quasi-GC labeling for standard 8QAM as shown in Fig. 7. Fig. 7 also shows the labels used in our simulations for star-8QAM, which is similar to the GC labels used in our simulations for 8PSK. For each 8-ary system, the overall bandwidth efficiency (throughput) using the $(15, 11)$ Hamming code and the accumulator code is 2.2 bits/sec/Hz. BER results for 8 iterations and 10 iterations are given for each of the four 8-ary systems.

In Fig. 10 we see that, at BER= 10^{-5} and for 10 iterations, with iterative demodulation and decoding exploring its inherent memory, NS-8QAM outperforms standard 8QAM having the same capacity by 0.5 dB, and standard 8QAM outperforms 8PSK by 0.2 dB. Note that at a throughput of 2.2 bits/sec/Hz, NS-8QAM and standard 8QAM

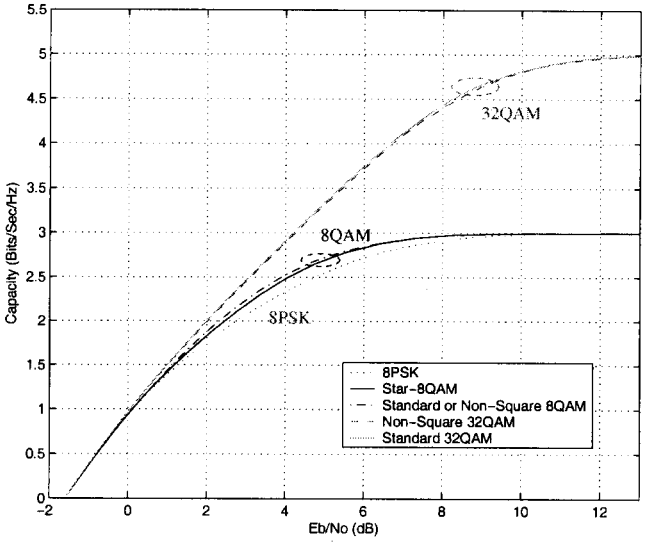

Fig. 9. Capacity comparison of the six different modulation schemes.

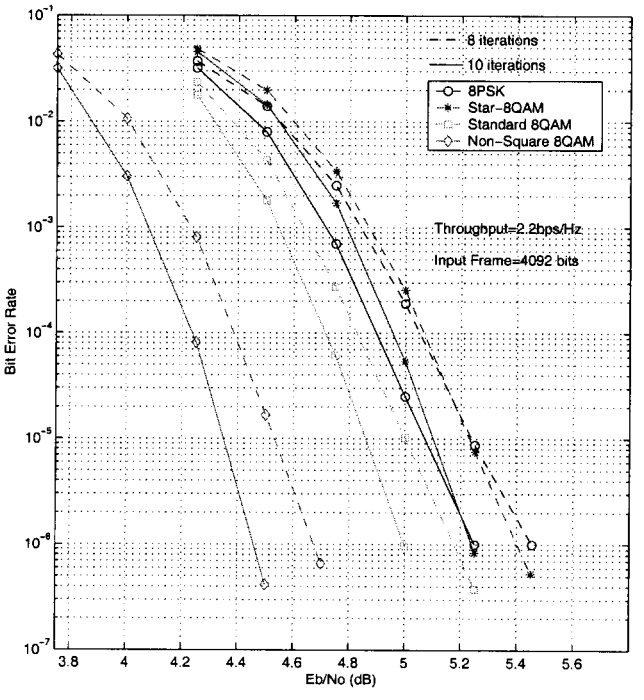

Fig. 10. BER comparison for coded NS-8QAM, star-8QAM, and 8PSK.

have a 0.6 dB capacity advantage compared to 8PSK, as demonstrated in Fig. 9 of Section IV-B. In addition, the minimum E_b/N_0 required to achieve this throughput for NS-8QAM is 2.87 dB. Since Fig. 10 shows that an E_b/N_0 of 4.35 dB is required for NS-8QAM to achieve BER= 10^{-5} with 10 iterations, this coded system with iterative demodulation and decoding is about 1.5 dB from the capacity of NS-8QAM.

Fig. 10 also shows the surprising fact that coded star-8QAM only has a performance similar to that of 8PSK, which is worse than standard 8QAM and much worse than NS-8QAM. This is in contrast to the uncoded case, where, as shown in Fig. 8, star-8QAM is about 1.6 dB better than 8PSK and about 0.24 dB better than standard 8QAM and NS-8QAM asymptotically. In addition, it is also in contrast to the fact that star-8QAM has about 0.43 dB capacity advantage compared to 8PSK at throughput 2.2 bits/sec/Hz. The reason that coded star-8QAM with iterative decoding does not perform well may be due to the fact that each of the four points on the inner circle of its constellation has four adjacent points with minimum distance, which makes it hard to come up with a good labeling system. Simulation results in Fig. 10 imply that the star-8QAM labels in Fig. 7 are probably not good enough to achieve the capacity advantage of star-8QAM over 8PSK, though our simulation results of an alternative labeling scheme (not shown here) were even worse. Labeling (or mapping) mechanisms suitable for iterative decoding processes are discussed in [25]–[28].

Fig. 11 shows the BER performance of coded NS-32QAM and standard 32QAM with quasi-GC labeling. The quasi-GC labeling for standard 32QAM is adopted from the labeling scheme demonstrated in "Case 1" of Fig. 15 in [21]. Again our simulation results are given for 8 iterations and 10 iterations. With 32QAM, the overall bandwidth efficiency of the coded system is 3.67 bits/sec/Hz. As shown on the capacity curves in Fig. 9, the minimum E_b/N_0 required to achieve this throughput for NS-8QAM is 5.85 dB, and it is 5.80 dB for standard 32QAM.

From Fig. 11 we see that, with iterative demodulation and decoding utilizing its inherent memory, NS-32QAM outperforms standard 32QAM by about 0.25 dB at BER= 10^{-5} with 10 iterations, and is about 1.8 dB from its capacity. Note that standard 32QAM has a slightly larger capacity than NS-32QAM, and it performs slightly better than NS-32QAM at large SNR in the uncoded case. Compared to the improvement of coded NS-8QAM over standard 8QAM, the smaller improvement of coded NS-32QAM over standard 32QAM may be due to the larger block length of the inherent SPC code in NS-32QAM. Specifically, for NS-32QAM, one parity-check bit is added for every five output bits of the accumulators, while for NS-8QAM, one parity-check bit is added for every three output bits of the accumulators.

VI. Conclusions

We have shown that NS-2^{2n+1}-QAM ($n \geq 1$) can be decomposed into an SPC encoder and a memoryless modulator in such a way that the inherent block encoder has a recursive nature. Therefore, NS-2^{2n+1}-QAM is by itself a form of coded modulation. When concatenated with an FEC code, we have described how to perform iterative demodulation and decoding to explore the inherent memory of NS-2^{2n+1}-QAM and its independent I and Q channel mapping and demapping. Comparisons of the capacity and BER/SER performance of coded and uncoded systems have been given for NS-8QAM and three other 8-ary modulations and for NS-32QAM and standard 32QAM. It

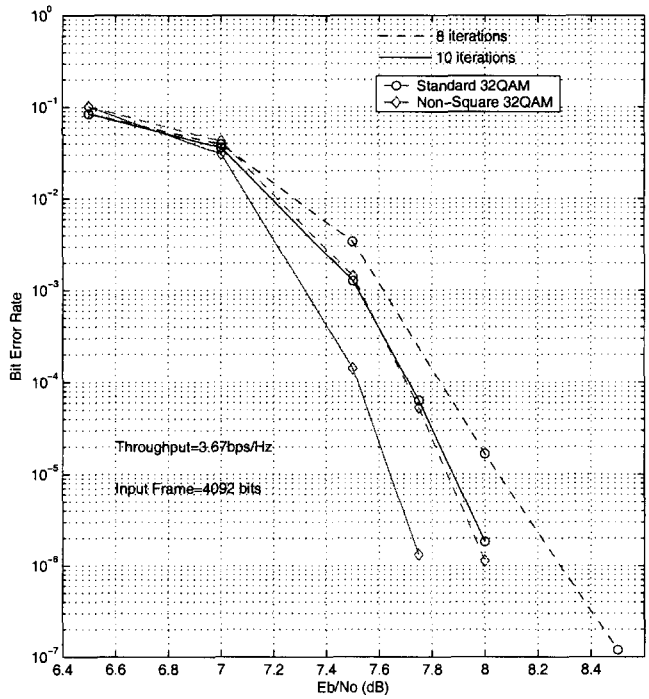

Fig. 11. BER comparison for coded NS-32QAM and standard 32QAM.

has been shown that NS-8QAM has the same capacity as standard 8QAM while NS-32QAM has a slightly smaller capacity than standard 32QAM. The star-8QAM has a smaller capacity than NS-8QAM, though its uncoded system has a better asymptotic SER performance. Simulation results show that, with iterative demodulation and decoding, coded NS-8QAM performs 0.5 dB better than standard 8QAM and 0.7 dB better than both 8PSK and star-8QAM at BER= 10^{-5}, when the FEC code is the $(15, 11)$ Hamming code concatenated with a rate-1 accumulator code, while coded NS-32QAM performs 0.25 dB better than standard 32QAM.

REFERENCES

[1] C. Berrou, A. Glavieux, and P. Thitimajshima, "Near Shannon limit error-correcting and decoding: Turbo codes (1)," in *Proc. IEEE Int. Conf. Commun. (ICC'93)*, vol. 2, Geneva, Switzerland, May 1993, pp. 23–26.

[2] S. Benedetto, D. Divsalar, G. Montorsi, and F. Pollara, "Serial concatenation of interleaved codes: performance analysis, design, and iterative decoding," in *The Telecommunications and Data Acuisition Progress Report*, vol. 42-126, Jet Propulsion Laboratory, Pasadena, CA, USA, Aug. 15, 1996. [Online]. Available: http://tmo.jpl.nasa.gov/tmo/progress'report/42-126/126D.pdf

[3] ——, "Serial concatenation of interleaved codes: performance analysis, design, and iterative decoding," *IEEE Trans. Inform. Theory*, vol. 44, no. 3, pp. 909–926, May 1998.

[4] C. Brutel, J. Boutros, and F. Belvèze, "Serial encoding and iterative detection of continuous phase modulations," in *Proc. IEEE Global Commun. Conf. (GLOBECOM'99)*, vol. 5, Rio de Janeireo, Brazil, Dec. 1999, pp. 2375–2379.

[5] K. R. Narayanan and G. L. Stüber, "Performance of trellis-coded CPM with iterative demodulation and decoding," *IEEE Trans. Commun.*, vol. 49, no. 4, pp. 676–687, Apr. 2001.

[6] P. Moqvist and T. M. Aulin, "Serially concatenated continuous phase modulation with iterative decoding," *IEEE Trans. Commun.*, vol. 49, no. 11, pp. 1901–1915, Nov. 2001.

[7] M. R. Shane and R. D. Wesel, "Parallel concatenated turbo codes for continuous phase modulation," in *Proc. IEEE Wireless Commun. Networking Conf. (WCNC'00)*, vol. 1, Chicago, IL, USA, Sept. 2000, pp. 147–152.

[8] M. Peleg and S. Shamai, "Iterative decoding of coded and interleaved noncoherent multiple symbol detected DPSK," *Electron. Lett.*, vol. 33, no. 12, pp. 1018–1020, June 1997.

[9] P. Hoeher and J. Lodge, ""Turbo DPSK": iterative differential PSK demodulation and channel decoding," *IEEE Trans. Commun.*, vol. 47, no. 6, pp. 837–843, June 1999.

[10] K. R. Narayanan and G. L. Stüber, "A serial concatenation approach to iterative demodulation and decoding," *IEEE Trans. Commun.*, vol. 47, no. 7, pp. 956–961, July 1999.

[11] P. S. K. Leung and K. Feher, "F-QPSK - a superior modulation technique for mobile and personal communications," *IEEE Trans. Broadcast.*, vol. 39, no. 2, pp. 288–294, June 1993.

[12] M. K. Simon and D. Divsalar, "A reduced-complexity, highly power-/bandwidth-efficient coded feher-patented quadrature-phase-shift-keying system with iterative decoding," in *The Telecommunications and Mission Operations Progress Report*, vol. 42-145, Jet Propulsion Laboratory, Pasadena, CA, USA, May 15, 2001. [Online]. Available: http://tmo.jpl.nasa.gov/tmo/progress_report/42-145/145A.pdf

[13] ——, "Further results on a reduced-complexity, highly power-/bandwidth-efficient coded feher-patented quadrature-phase-shift-keying system with iterative decoding," in *The Interplanetary Network Progress Report*, vol. 42-146, Jet Propulsion Laboratory, Pasadena, CA, USA, Aug. 15, 2001. [Online]. Available: http://tmo.jpl.nasa.gov/tmo/progress_report/42-146/146I.pdf

[14] ——, "A reduced complexity highly power/bandwidth efficient coded FQPSK system with iterative decoding," in *Proc. IEEE Int. Conf. Commun. (ICC'01)*, vol. 7, Helsinki, Finland, June 2001, pp. 2204–2210.

[15] D. Divsalar and S. Dolinar, "Concatenation of Hamming codes and accumulator codes with high-order modulations for Gbps decoding," Submitted to IEEE Global Commun. Conf. (Globecom'03), San Francisco, CA, USA, Dec. 2003.

[16] J. A. Torres, "Method for using non-squared QAM constellations," Forum Contribution, IEEE 802.16 Broadband Wireless Access Working Group, May 23, 2002. [Online]. Available: http://www.ieee802.org/16/tga/contrib/C80216a-02_66.pdf

[17] S. Benedetto, D. Divsalar, G. Montorsi, and F. Pollara, "A soft-input soft-output maximum a posteriori (MAP) module to decode parallel and serial concatenated codes," in *The Telecommunications and Data Acuisition Progress Report*, vol. 42-127, Jet Propulsion Laboratory, Pasadena, CA, USA, Nov. 15, 1996. [Online]. Available: http://tmo.jpl.nasa.gov/tmo/progress_report/42-127/127H.pdf

[18] ——, "A soft-input soft-output APP module for iterative decoding of concatenated codes," *IEEE Commun. Lett.*, vol. 1, no. 1, pp. 22–24, Jan. 1997.

[19] L. R. Bahl, J. Cocke, F. Jelinek, and J. Raviv, "Optimal decoding of linear codes for minimizing symbol error rate," *IEEE Trans. Inform. Theory*, vol. IT-20, no. 2, pp. 284–287, Mar. 1974.

[20] A. Ambroze, G. Wade, and M. Tomlinson, "Iterative MAP decoding for serial concatenated convolutional codes," *IEE Proc.-Commun.*, vol. 145, no. 2, pp. 53–59, Apr. 1998.

[21] R. D. Wesel, X. Liu, J. M. Cioffi, and C. Komninakis, "Constellation labeling for linear encoders," *IEEE Trans. Inform. Theory*, vol. 47, no. 6, pp. 2417–2431, Feb. 2001.

[22] J. G. Proakis, *Digital Communications*, 2nd ed. McGraw-Hill, 1989, p. 281.

[23] S. Benedetto and E. Biglieri, *Principles of Digital Transmission: With Wireless Applications*. New York: Kluwer Academic/Plenum Press, 1999, p. 196.

[24] R. E. Blahut, *Principles and Practice of Information Theory*. Addison-Wesley, 1990, p. 275.

[25] A. Gorokhov and M. van Dijk, "Optimised labeling maps for bit-interleaved transmission with turbo demodulation," in *Proc. IEEE Veh. Tech. Conf. (VTC'01)*, vol. 2, Rhodes, Greece, May 2001, pp. 1459–1463.

[26] J. Tan and G. Stüber, "Analysis and design of interleaver mappings for iteratively decoded BICM," in *Proc. IEEE Int. Conf. Commun. (ICC'02)*, vol. 3, 2002, pp. 1403– 1407.

[27] S. ten Brink, J. Speidel, and R.-H. Yan, "Iterative demapping for QPSK modulation," *Electron. Lett.*, vol. 34, no. 15, pp. 1459–1460, July 1998.

[28] ——, "Iterative demapping and decoding for multilevel modulation," in *Proc. IEEE Global Commun. Conf. (GLOBECOM'98)*, vol. 1, Sydney, NSW, Australia, Nov. 1998, pp. 579–584.